Universal Correlations in a Nonlinear Periodic 1D System

Yaron Silberberg,[1,*] Yoav Lahini,[1] Yaron Bromberg,[1] Eran Small,[1] and Roberto Morandotti[2]
[1]*Department of Physics of Complex Systems, Weizmann Institute of Science, Rehovot 76100, Israel*
[2]*Institute National de la Recherche Scientifique, Varennes, Québec, Canada*
(Received 1 December 2008; published 12 June 2009)

When a periodic 1D system described by a tight-binding model is uniformly initialized with equal amplitudes at all sites, yet with completely random phases, it evolves into a thermal distribution with no spatial correlations. However, when the system is nonlinear, correlations are spontaneously formed. We find that for strong nonlinearities, the intensity histograms approach a narrow Gaussian distributed around their mean and phase correlations are formed between neighboring sites. Sites tend to be out of phase for a positive nonlinearity and in phase for a negative one. Most impressively, the field correlation takes a universal shape independent of parameters. These results are relevant to bosonic gas in 1D optical lattices as well as to nonlinear optical waveguide arrays, which are used to demonstrate experimentally some of the features of this equilibrium state.

DOI: 10.1103/PhysRevLett.102.233904 PACS numbers: 42.65.Sf, 42.25.Dd, 42.65.Tg

The tight-binding approximation is one of the simplest models that predict band structure and ballistic motion in periodic systems [1]. Using a tight-binding model with disorder, P. W. Anderson was able to predict and study the effect of localization in disordered lattices [2]. A nonlinear version of the tight-binding model, better known as the Discrete Nonlinear Schrödinger Equation (DNLSE), has been used to study nonlinear evolution in periodic systems, initially in the context of periodic molecular and mechanical systems [3], and extensively in recent years to describe nonlinear propagation in optical waveguide lattices [4,5], as well as matter waves in light-induced lattices [6]. In particular, the DNLSE explains the formation of nonlinear intrinsic localized modes, also known as discrete solitons [7] or discrete breathers [8].

Here, we report on a new phenomenon that occurs in periodic systems, in the limit of strong nonlinearity. What we find is that when the system is initialized with random-phase fields, it evolves into particular distributions with well-defined stationary statistical properties. Most interestingly, the field correlation function and the distribution of phases assume universal forms independent of the exact value of the nonlinear parameter. The resulting distribution induces a dynamic structure with several intriguing properties.

This system is particularly relevant to recent theory [9] and experiments [10] with ultracold bosonic matter in a one-dimensional potential. These studies show that phase coherence builds up when bosonic matter, prepared initially in a highly number-squeezed Mott-insulating state, is allowed to interact via a sudden reduction of the lattice potential. These works investigated the interesting dynamics related to the buildup of coherence in the superfluid regime, but have not discussed the unique properties of the equilibrium state that is eventually reached and its universality. We show that this state can be interrogated experimentally by the study of the equivalent optical system.

In Fig. 1, we show the results of an optical experiment in a waveguide array that motivated this study. Light with uniform intensity yet random phases was injected into a large number of waveguides in a periodic AlGaAs waveguide lattice [4,5,11]. The light source was a pulsed optical parametric amplifier, producing 1.2 ps pulses at a wavelength of 1530 nm with a 1 kHz repetition rate. The laser beam was shaped to couple to 15 waveguides, and the spatial phase of each input was randomized using a

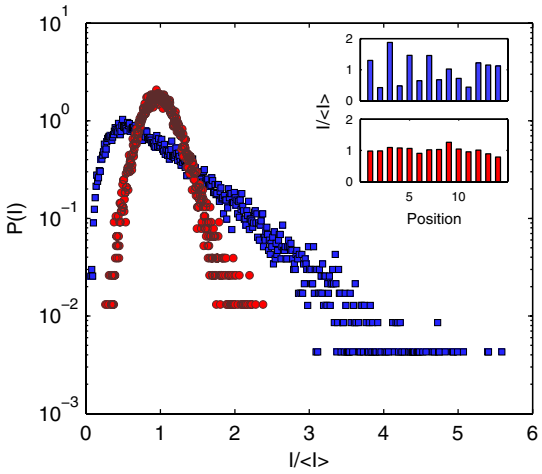

FIG. 1 (color online). Experimental measurement of output light intensities from a waveguide array, when input fields with equal amplitudes, yet random phases, are coupled to several adjacent waveguides. The measured intensity values of many random-phase realizations are shown as histograms for linear propagation (blue squares) and high-intensity, nonlinear propagation (red circles). The output intensity distribution is exponential-like in the linear propagation and becomes narrow, Gaussian-like in the nonlinear case. Inset: Two sets of measurements for an input with the same phase realization after linear (top panel) and nonlinear (bottom panel) propagation, showing that the intensity fluctuations are reduced in the nonlinear case.

computer-controlled spatial light modulator. The intensity at the output end was measured, and the histograms of intensity values obtained from many repeats of the experiment with different random-phase realizations are shown for both low-intensity (linear) and high-intensity (nonlinear) light. While linear propagation produced exponential-like distribution of intensities, as expected for summing of many random-phase inputs, the nonlinear propagation yielded a much narrower distribution around the average intensity, as shown in Fig. 1. Increasing the optical power led to the narrowing of the output distribution. Note that for both measurements, the counts at low intensity values are underestimated because of scattered light and instrumentation noise.

To investigate this behavior, we have modeled the problem using the DNLSE. While we use here the notations of optics, our results hold in general for all other systems described by the DNLSE. Light evolution in a periodic array of weakly coupled waveguides is described by

$$i\frac{da_n}{dz} = C(a_{n-1} + a_{n+1}) + \gamma|a_n|^2 a_n, \tag{1}$$

where a_n is the amplitude of the mode in the nth waveguide, C is the coupling coefficient to the nearest neighbors, and γ is the nonlinear coefficient, positive (negative) for focusing (defocusing) nonlinearity. We shall consider the situation where light is injected into the array with uniform amplitudes $|a_n| = a_0$, yet with completely uncorrelated, random phases. It is convenient to use the normalized equation,

$$i\frac{du_n}{d\zeta} = (u_{n-1} + u_{n+1}) + \Gamma|u_n|^2 u_n, \tag{2}$$

where $\zeta = zC$, $u_n = a_n/a_0$, and $\Gamma = \gamma a_0^2/C$. With this normalization, the input intensities are all uniform with $I_n(0) = u_n u_n^* = 1$.

Consider first the linear problem, i.e., $\Gamma = 0$. As might be expected, after a certain distance, mixing of the different input fields leads to an output pattern with fluctuating intensities. Figures 2(a)–2(c) shows results of numerical simulations of Eq. (2) for various properties of the fields after propagating a distance of $\zeta = 10$ in an array with $N = 256$ sites. Periodic boundary conditions are used to avoid edge effects. The results shown are averaged over 500 realizations with different random initial fields. Figure 2(a) shows the intensity histogram; it follows an exponential law, $P(I) = \exp(-I)$, as expected for random fields. Figure 2(b) shows the field correlations $C_k = \sum(u_n u_{n+k}^* + u_n^* u_{n+k})/2N$ demonstrating, as could be expected, that the fields at different sites do not correlate. Finally, Fig. 2(c) shows the histogram of phase differences between neighbors, $\theta_n = \phi_n - \phi_{n+1}$, with $\phi_n = \arg(u_n)$ the phase of the field u_n. These phases are uniformly distributed.

We now repeat the simulations with nonlinearity, and we will be interested mostly in the limit of strong nonlinearity; results for $\Gamma = \pm 20$ and for $\Gamma = \pm 200$ are given in Figs. 2(d)–2(f). Two differences from the linear case are obvious. First, the intensity histograms, shown in Fig. 2(d), now converge around the average intensity value of 1, with a width that shrinks with the nonlinear parameter. The distribution seems to fit well a Gaussian distribution with $P(I) = \exp[-(I-1)^2/2\sigma^2]$, and it is independent of the sign of the nonlinearity.

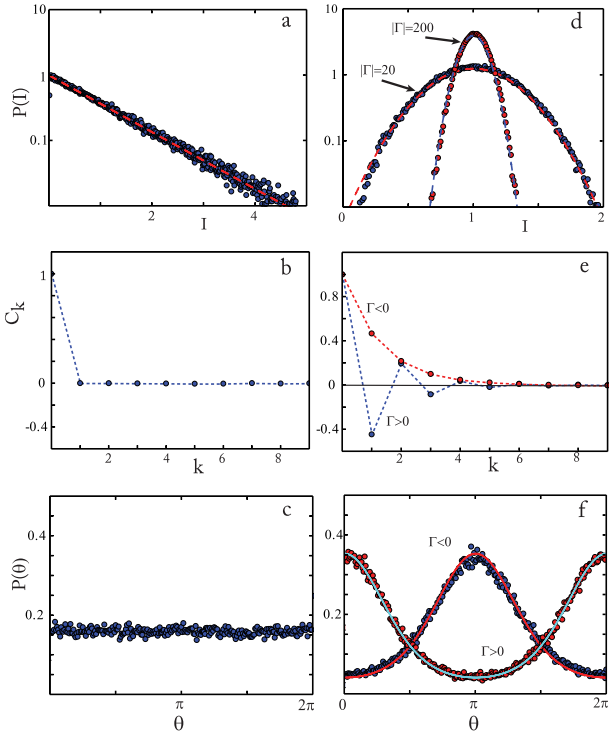

FIG. 2 (color online). Simulation results of the DNLSE with uniform intensities and random phases. (a) Intensity histogram, (b) field correlation, and (c) phase-difference histogram for a linear system ($\Gamma = 0$), exhibiting exponential intensity distribution and uncorrelated fields and phases. (d) Intensity histograms for $\Gamma = \pm 20$ (blue circles) and $\Gamma = \pm 200$ (red circles). The distributions are narrower at higher nonlinearities, yet independent of the sign of Γ. (e) The universal field correlation function is identical for both nonlinear values, but depends on their sign: blue for positive (focusing, $\Gamma > 0$), red for negative nonlinearities. (f) Phase-difference histograms also approach a universal distribution, concentrating around π for positive nonlinearity and 0 for the negative case. The theoretical lines in (d)–(f) are predictions of Eqs. (7) and (8).

The second major effect of the nonlinearity is the induced spatial field correlations. Most interestingly, the correlation function [Fig. 2(e)] takes a shape that is independent of the nonlinearity value, and is sensitive only to its sign. It is described well by exponential decays, $C_k = (-1)^k \exp(-\alpha k)$ for positive (focusing) nonlinearity and $C_k = \exp(-\alpha k)$ for the negative case. Note that the correlation is only visible in the fields—the intensities remain uncorrelated; intensity correlations show a diminished peak at $k = 0$ and a uniform background. These field patterns are consistent with the known properties of modu-

lation instability in such systems: Staggered (unstaggered) fields are stable in positive (negative) nonlinearity arrays [12].

Since the intensities become more uniform at high nonlinearities, the field correlation functions are dictated by the variations of phases between neighboring sites. In Fig. 2(f), we show the histograms of these phase differences for positive and negative nonlinearities. While in the former, neighboring waveguides are most likely to be out of phase, as the distribution peaks at π, in the latter, neighboring waveguides tend to be in phase. This distribution of phases also attains a constant profile at high-nonlinearity values.

The field correlations and the intensity distributions are closely related. This can be deduced from the conserved quantities,

$$H = \frac{1}{2}\Gamma \sum I_n^2 + \sum (u_n u_{n+1}^* + u_n^* u_{n+1}) \tag{3}$$

$$A = \sum I_n, \tag{4}$$

which represent the equivalent Hamiltonian and the total photon number, respectively.

From these it is easy to show that

$$\frac{\Gamma}{4}\sigma^2(\zeta) + C_1(\zeta) = H_0 \tag{5}$$

is also constant. Here, $\sigma = (\Sigma I_n^2/N - 1)^{1/2}$ is the standard deviation of the intensities. Since our initial condition are of uniform intensities, $\sigma^2(0) = 0$, and random phases, $C_1(0) \approx 0$, then $H_0 = 0$; hence,

$$\frac{\Gamma}{4}\sigma^2(\zeta) = -C_1(\zeta). \tag{6}$$

Equation (6) predicts that the signs of C_1 and Γ are different, as indeed is observed in Fig. 2. For weak nonlinearity ($\Gamma \ll 1$), when the distribution deviates only slightly from exponential, a small correlation is formed with $C_1 = -\Gamma/4$. However, as the nonlinearity increases, Eq. (6) predicts that the intensity distribution has to narrow down, since necessarily $|C_1| < 1$.

To relate the phase and intensity fluctuations, we have to study the statistical properties of the DNLSE. Such investigations were carried out by Rasmussen *et al.* [13], and extended later by Rumpf [14]. They were mostly interested in the conditions for the generation of localized structures. With our initial conditions, it can be shown that localized structures are not formed, but we can use the same formalism to derive the probability distributions for phase and intensities.

In essence, the state of maximal entropy $S[p(I_1, \ldots I_N, \theta_1, \ldots \theta_N)] = -\int p \ln p \prod dI_i d\theta_i$ can be derived by the variational problem $\delta(S - \alpha A - \eta H - \lambda \int p) = 0$, where α, η, and λ are the appropriate Lagrange multipliers [14]. In the limit of $\Gamma \gg 1$, it can be shown that $\sum (u_n u_{n+1}^* + \text{c.c.}) \approx 2 \sum \cos(\theta_n)$ [15]. This is also consistent with the observation that the intensities are uncorrelated, and at high nonlinearities, they are close to their average value of 1. With this approximation, also known as the quantum phase model [15], the intensities and phases are separable, and their distributions are derived to be

$$p_I(I) = \lambda_1 \exp\left[-\frac{\eta\Gamma}{2}(I-1)^2\right] \tag{7}$$

$$p_\theta(\theta) = \lambda_2 \exp[-2\eta \cos(\theta)] \tag{8}$$

with λ_1, λ_2 appropriate normalization constants and $\eta \approx \pm 0.533$ is the solution of $4\eta \int \cos(\theta) p_\theta(\theta) d\theta + 1 = 0$, where the sign is selected to match the sign of Γ. The phase distribution is then maximized at $\theta = \pi$ ($\theta = 0$) for positive (negative) Γ, respectively. Note that these universal phase distribution functions, which are shown as lines in Fig. 2(f), are independent of the value of the nonlinearity. They lead to the universal correlation function that decays with $C_k/C_{k+1} = -4\eta$ as shown in Fig. 2(e).

The strong nonlinear effect described in this Letter introduces strong deformations to the lattice. One way to characterize these deformations is to investigate the transport properties of a weak probe field, which propagates in the lattice simultaneously with the strong field that induces the nonlinear effect. The probe field does not interfere with the strong field, but it is driven by the potential $\Gamma I_n \equiv V_n(\zeta)$, where I_n is the intensity of the *strong* beam at nth waveguide. The propagation of the probe field can be described by a linear set of equations, in which V_n is an external potential. Such an approach can yield additional insight by translating the problem into a more familiar linear evolution. In our case, the equivalent linear problem is that of diagonal disorder: The potential V_n fluctuates from site to site, and it is also changing dynamically with ζ. While we have shown above that the variations in intensities tend to diminish at high nonlinearities [$\sigma = (\eta\Gamma)^{-1/2}$], the variations in the induced potential, i.e., $\Gamma\sigma$ actually increase. The array becomes effectively more disordered: A stationary (i.e., ζ-independent) structure with this level of disorder would have been characterized by a localization length that is narrower than the lattice spacing. However, this increase in disorder is also accompanied by faster dynamics: The induced pattern changes faster at higher nonlinearities. The induced potential map $V_n(\zeta)$ is shown in Fig. 3, together with the correlation maps $Y(k, \delta\zeta) = \Sigma_n \int d\zeta V_n(\zeta) V_{n-k}(\zeta - \delta\zeta)$. Note that while at a given ζ the potentials (and intensities) at adjacent sites do not correlate, $Y(k, 0) = \delta_{k,0}$, they are correlated at other values of ζ. It is this dynamic potential structure that determines the field correlations and other peculiarities of this system.

We have simulated the simultaneous propagation of a strong nonlinear field and a weak probe field in an array with 1024 sites. The strong field is simulated as described above, and the probe is launched into a single central site at $\zeta = 0$. Figure 4(a) shows the width of the probe beam, averaged over several realizations, as a function of $\zeta^{1/2}$, for

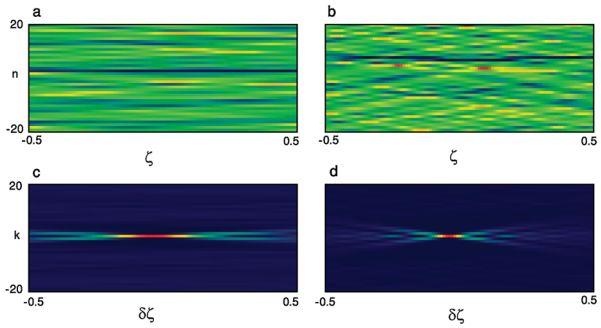

FIG. 3 (color online). Maps of the potential V_n induced by the fluctuating fields for (a) $\Gamma = 20$ and (b) $\Gamma = 200$ and the corresponding correlation maps $Y(k, \delta\zeta)$ (c), (d). The maps show a section of 40 waveguides (vertically) and a propagation of $\zeta = 1$. Note the faster dynamics for the higher nonlinearity, evident also in the correlation map. For easy viewing, the potentials are normalized to their peaks, although the values in (b) are about 3 times higher than in (a).

two values of nonlinearity, $\Gamma = 20$ and $\Gamma = 200$. Figure 4(b) shows the probe intensity distribution at $\zeta = 2000$. It seems that the broadening is governed mostly by diffusive dynamics, that is, a Gaussian-like distribution that broadens diffusively as $\zeta^{1/2}$. Indeed, dynamic disorder that is spatially uncorrelated is known to lead to diffusive broadening [16–18]. What we find interesting is that at higher nonlinearities, the diffusion coefficient is actually larger, in spite of the stronger disorder. This is most likely the result of the faster dynamics, but it could be that the nontrivial correlation maps also plays a role. These points are currently under investigation.

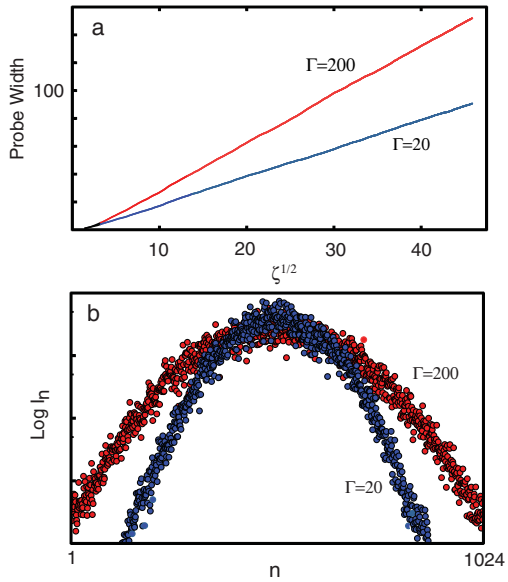

FIG. 4 (color online). The diffusion of a weak probe in the potential induced by the high-intensity fluctuating field with $\Gamma = 20$ and $\Gamma = 200$. (a) the averaged probe width as a function of $\zeta^{1/2}$. (b) The averaged probe profile at $\zeta = 2000$.

In conclusion, we have shown that when systems described by the DNLSE are initialized with equal amplitudes yet random phases, universal field correlations are formed in the high-nonlinearity limit. In contrast with the thermal distribution of intensities obtained in linear propagation, the intensity variations are diminished, and universal phase correlations are formed. These results are relevant to two experimental situations; in optics, the physics of nonlinear waveguide arrays and, in quantum gases, for systems switched from Mott insulators to superfluidity. It is worth noting that the fact that these systems relax to equilibrium while maximizing entropy [19] is closely related to their discrete nature. Continuous, integrable 1D systems do not generally display ergodicity [20] and may not be amiable to similar statistical physics analysis.

We thank E. Altman and A. Polkovnikov for illuminating discussions and R. Helsten for valuable help. This work was supported by the German-Israel Foundation (GIF) and the Crown Photonic Center.

*yaron.silberberg@weizmann.ac.il

[1] F. Bloch, Z. Phys. **52**, 555 (1929).
[2] P. Anderson, Phys. Rev. **109**, 1492 (1958).
[3] J. C. Eilbeck, P. S. Lomdahl, and A. C. Scott, Physica D (Amsterdam) **16** 318 (1985).
[4] F. Lederer *et al.*, Phys. Rep. **463**, 1 (2008).
[5] D. N. Christodoulides, F. Lederer, and Y. Silberberg, Nature (London) **424**, 817 (2003).
[6] A. Trombettoni and A. Smerzi, Phys. Rev. Lett. **86**, 2353 (2001).
[7] D. N. Christodoulides and R. I. Joseph, Opt. Lett. **13**, 794 (1988).
[8] S. Flach and C. R. Willis, Phys. Rep. **295**, 181 (1998).
[9] A. Polkovnikov, S. Sachdev, and S. M. Girvin, Phys. Rev. A **66**, 053607 (2002).
[10] A. K. Tuchman, C. Orzel, A. Polkovnikov, and M. A. Kasevich, Phys. Rev. A **74**, 051601(R) (2006).
[11] H. S. Eisenberg, Y. Silberberg, R. Morandotti, A. R. Boyd, and J. S. Aitchison, Phys. Rev. Lett. **81**, 3383 (1998).
[12] J. Meier *et al.*, Phys. Rev. Lett. **92**, 163902 (2004).
[13] R. O. Rasmussen, T. Cretegny, and P. G. Kevrekidis, Phys. Rev. Lett. **84**, 3740 (2000).
[14] B. Rumpf, Phys. Rev. E **77**, 036606 (2008).
[15] S. D. Huber *et al.*, Phys. Rev. Lett. **100**, 050404 (2008).
[16] A. Madhukar and W. Post, Phys. Rev. Lett. **39**, 1424 (1977).
[17] N. Lebedev, P. Maass, and S. Feng, Phys. Rev. Lett. **74**, 1895 (1995).
[18] A. Amir *et al.*, Phys. Rev. E **79**, 050105 (2009).
[19] M. Cramer, C. M. Dawson, J. Eisert, and T. J. Osborne, Phys. Rev. Lett. **100**, 030602 (2008).
[20] T. Kinoshita, T. Wenger, and D. S. Weiss, Nature (London) **440**, 900 (2006).